

# Measurement of the ${}^3\text{He}(e, e'p)pn$ reaction at high missing energies and momenta

F. Benmokhtar,<sup>1,2</sup> M. M. Rvachev,<sup>3</sup> E. Penel-Nottaris,<sup>4</sup> K. A. Aniol,<sup>5</sup> W. Bertozzi,<sup>3</sup> W. U. Boeglin,<sup>6</sup> F. Butaru,<sup>4</sup> J. R. Calarco,<sup>7</sup> Z. Chai,<sup>3</sup> C. C. Chang,<sup>8</sup> J. -P. Chen,<sup>9</sup> E. Chudakov,<sup>9</sup> E. Cisbani,<sup>10</sup> A. Cochran,<sup>11</sup> J. Cornejo,<sup>5</sup> S. Dieterich,<sup>1</sup> P. Djawotho,<sup>12</sup> W. Duran,<sup>5</sup> M. B. Epstein,<sup>5</sup> J. M. Finn,<sup>12</sup> K. G. Fissum,<sup>13</sup> A. Frahi-Amroun,<sup>2</sup> S. Frullani,<sup>10</sup> C. Furget,<sup>4</sup> F. Garibaldi,<sup>10</sup> O. Gayou,<sup>12</sup> S. Gilad,<sup>3</sup> R. Gilman,<sup>1,9</sup> C. Glashauser,<sup>1</sup> J.-O. Hansen,<sup>9</sup> D. W. Higinbotham,<sup>3,9</sup> A. Hotta,<sup>14</sup> B. Hu,<sup>11</sup> M. Iodice,<sup>10</sup> R. Iomni,<sup>10</sup> C. W. de Jager,<sup>9</sup> X. Jiang,<sup>1</sup> M. K. Jones,<sup>9,8</sup> J. J. Kelly,<sup>8</sup> S. Kox,<sup>4</sup> M. Kuss,<sup>9</sup> J. M. Laget,<sup>15</sup> R. De Leo,<sup>16</sup> J. J. LeRose,<sup>9</sup> E. Liatard,<sup>4</sup> R. Lindgren,<sup>17</sup> N. Liyanage,<sup>9</sup> R. W. Lourie,<sup>18</sup> S. Malov,<sup>1</sup> D. J. Margaziotis,<sup>5</sup> P. Markowitz,<sup>6</sup> F. Merchez,<sup>4</sup> R. Michaels,<sup>9</sup> J. Mitchell,<sup>9</sup> J. Mougey,<sup>4</sup> C. F. Perdrisat,<sup>12</sup> V. A. Punjabi,<sup>19</sup> G. Quémener,<sup>4</sup> R. D. Ransome,<sup>1</sup> J.-S. Réal,<sup>4</sup> R. Roché,<sup>20</sup> F. Sabatié,<sup>21</sup> A. Saha,<sup>9</sup> D. Simon,<sup>21</sup> S. Strauch,<sup>1</sup> R. Suleiman,<sup>3</sup> T. Tamae,<sup>22</sup> J. A. Templon,<sup>23</sup> R. Tieulent,<sup>4</sup> H. Ueno,<sup>24</sup> P. E. Ulmer,<sup>21</sup> G. M. Urciuoli,<sup>10</sup> E. Voutier,<sup>4</sup> K. Wijesooriya,<sup>25</sup> and B. Wojtsekhowski<sup>9</sup>

(Jefferson Lab Hall A Collaboration)

<sup>1</sup>Rutgers, The State University of New Jersey, Piscataway, New Jersey 08854, USA

<sup>2</sup>Université des Sciences et de la Technologie, BP 32, El Alia, Bab Ezzouar, 16111 Alger, Algérie

<sup>3</sup>Massachusetts Institute of Technology, Cambridge, Massachusetts 02139, USA

<sup>4</sup>Laboratoire de Physique Subatomique et de Cosmologie, F-38026 Grenoble, France

<sup>5</sup>California State University, Los Angeles, Los Angeles, California 90032, USA

<sup>6</sup>Florida International University, Miami, Florida 33199, USA

<sup>7</sup>University of New Hampshire, Durham, New Hampshire 03824, USA

<sup>8</sup>University of Maryland, College Park, Maryland 20742, USA

<sup>9</sup>Thomas Jefferson National Accelerator Facility, Newport News, Virginia 23606, USA

<sup>10</sup>INFN, Sezione Sanità and Istituto Superiore di Sanità, Laboratorio di Fisica, I-00161 Rome, Italy

<sup>11</sup>Hampton University, Hampton, Virginia 23668, USA

<sup>12</sup>College of William and Mary, Williamsburg, Virginia 23187, USA

<sup>13</sup>University of Lund, Box 118, SE-221 00 Lund, Sweden

<sup>14</sup>University of Massachusetts, Amherst, Massachusetts 01003, USA

<sup>15</sup>CEA-Saclay, F-91191 Gif Sur-Yvette Cedex, France

<sup>16</sup>INFN, Sezione di Bari and University of Bari, I-70126 Bari, Italy

<sup>17</sup>University of Virginia, Charlottesville, Virginia 22901, USA

<sup>18</sup>State University of New York at Stony Brook, Stony Brook, New York 11794, USA

<sup>19</sup>Norfolk State University, Norfolk, Virginia 23504, USA

<sup>20</sup>Florida State University, Tallahassee, Florida 32306, USA

<sup>21</sup>Old Dominion University, Norfolk, Virginia 23529, USA

<sup>22</sup>Laboratory of Nuclear Science, Tohoku University, Sendai 982-0826, Japan

<sup>23</sup>University of Georgia, Athens, Georgia 30602, USA

<sup>24</sup>Yamagata University, Kojirakawa-machi 1-4-12, Yamagata 990-8560, Japan

<sup>25</sup>University of Illinois, Champaign-Urbana, Illinois 61801, USA

(Dated: June 4, 2018)

Results of the Jefferson Lab Hall A quasi-elastic  ${}^3\text{He}(e, e'p)pn$  measurements are presented. These measurements were performed at fixed transferred momentum and energy,  $q = 1502$  MeV/c and  $\omega = 840$  MeV, respectively, for missing momenta  $p_m$  up to 1 GeV/c and missing energies in the continuum region, up to pion threshold; this kinematic coverage is much more extensive than that of any previous experiment. The cross section data are presented along with the effective momentum density distribution and compared to theoretical models.

PACS numbers: 25.30.Fj, 21.45+v, 24.85.+p, 27.10.+h

The role of correlations in nuclear structure remains a topic of primary importance. On the theoretical side, it is clear that correlations in the nuclear wave function must exist. The question is whether correlations can be understood as arising from the  $NN$  force and three-body forces, or whether it will be necessary to invoke quark degrees of freedom. However, the role of correlations in the available experimental data is often obscure. Attempts to make more definitive measurements with exclusive  $(e, e'p)$  or  $(e, e'NN)$  measurements suffer

from reaction mechanism ambiguities; physics such as meson-exchange currents (MEC), isobar configurations (IC), and final-state interactions (FSI) mask the effects of correlations. Better experimental data are needed for a definitive conclusion.

In this letter, we present an attempt to improve the study of correlations, using the  ${}^3\text{He}(e, e'p)pn$  reaction. The measurements are in kinematics designed to suppress the effects of some of the complicating underlying physics and enhance correlations. In particular, we choose high

four-momentum transfer  $Q^2$  to suppress MEC and to get a resolution smaller than the nucleon size, quasifree kinematics  $x \approx 1$  to suppress IC, and the continuum three-body breakup (3bbu) channel. A recent study [1] of  $^{16}\text{O}(e, e'p)X$  demonstrates the greater kinematic coverage and statistical precision achievable with the current generation of accelerator facilities; the results presented here for the  $^3\text{He}(e, e'p)pn$  reaction are by a large margin the most comprehensive, high resolution, experimental investigation of the continuum region.

To further motivate the studies presented, in particular the choice of the 3bbu channel, we present two signatures of  $NN$  correlations in  $^3\text{He}$  that one might expect to observe in the  $(e, e'p)$  reaction, in the absence of complicating reaction mechanisms. Consider two correlated nucleons, which in their center of mass system have equal and opposite momenta,  $\pm\vec{p}_c$ , with higher momenta reflecting smaller separations. An electron scattering on a proton belonging to such a correlated pair inside  $^3\text{He}$  [2, 3] transfers energy  $\omega$  and momentum  $\vec{q}$ . If the spectator nucleon is at rest, the struck proton is ejected with momentum  $\vec{q} - \vec{p}_c$ , while the other nucleon of the pair moves off with the recoil momentum of the reaction,  $\vec{p}_c$ . The spectator nucleon and the undetected nucleon of the pair constitute a recoil system of mass:

$$M_r^2 = \left[ M_{spec} + \sqrt{M_N^2 + p_c^2} \right]^2 - p_c^2. \quad (1)$$

Here  $M_N$  is the nucleon mass and  $M_{spec}$  is the mass of the spectator nucleon. Thus, in this simple reaction mechanism picture, a signature of correlations is a peak in the 3bbu cross section as a function of missing energy,  $E_m$ , with the position depending on  $p_c$ :  $E_m = M_r + M_p - M_{^3\text{He}}$ . The peak width reflects the motion of the center of mass with respect to the spectator nucleon.

The total strength of the correlation peak as a function of momentum yields a second signature of  $NN$  correlations. While we expect  $NN$  correlations to generally be more important at missing momenta greater than the Fermi momentum, the 3bbu strength will be enhanced relative to that for 2bbu as missing momentum increases due to a reduced probability for the two undetected nucleons to form a bound deuteron at high  $p_c$ .

An apparent correlation peak in the continuum was observed with limited statistics and limited kinematic range for the first time at Saclay [4], on  $^3\text{He}$ , and subsequently on  $^4\text{He}$  [5]. Simply interpreting the data as evidence for correlations, as suggested by the simple reaction mechanism picture of Fig. 1a, neglects the complications of MEC, IC, and FSI. In particular, the derivation of the peak position is purely kinematic, and the peak can appear as long as the electrodisintegration involves two active nucleons plus spectator nucleons. Thus, when the two nucleons in the active pair rescatter, Fig. 1b, the position and width of the peak do not change, and the

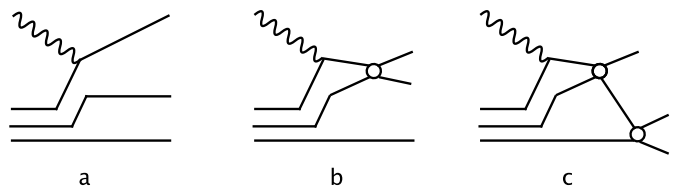


FIG. 1: Feynman diagrams for a) direct disintegration, b) rescattering, and c) rescattering with the spectator nucleon.

simple picture remains valid, but one measures the transition between a correlated pair in the ground state and a correlated pair in the continuum. But when one of the nucleons of the active pair re-interacts with the spectator third nucleon, Fig. 1c, the position, shape, and amplitude of the peak might all be affected. Rescattering also makes the measured missing momentum  $p_m$  different from the correlation momentum  $p_c$ , so it is clear then that the observed momentum distribution does not simply reflect the nuclear wave function – it is not an actual density. The lack of an apparent correlation peak in continuum  $(e, e'p)$  on heavier nuclei, e.g.,  $^{16}\text{O}$  [1], is believed to result from the small probability of having only two active nucleons when the number of spectators gets large.

In Thomas Jefferson National Accelerator Facility (JLab) Hall A experiment E89-044 [6], we studied the  $^3\text{He}(e, e'p)$  reaction in the quasi-elastic region at transferred 3-momentum  $|\vec{q}| = 1502$  MeV/c and energy  $\omega = 840$  MeV, so  $Q^2 = 1.55$  GeV<sup>2</sup>. This paper reports the results of measurements in perpendicular kinematics with Bjorken  $x = 0.98$ , near the top of the quasifree peak. Protons were detected at several angles relative to  $\vec{q}$ , corresponding to missing momenta  $p_m$  of 0 - 1 GeV/c. Results of the  $^3\text{He}(e, e'p)d$  reaction channel from this experiment were reported in [7]; here we focus on the continuum  $^3\text{He}(e, e'p)pn$  channel,  $E_m > 7.72$  MeV.

A continuous,  $\approx 120$   $\mu\text{A}$ , electron beam was scattered from  $^3\text{He}$  in a 10 cm diameter cylindrical cell, mounted with the beam passing through the center of the target perpendicular to the symmetry axis. The  $^3\text{He}$  target density was  $\approx 0.072$  g/cm<sup>3</sup> [7]. The scattered electrons and knocked-out protons were detected in the two High-Resolution Spectrometers (HRS<sub>e</sub> and HRS<sub>h</sub>). Details of the Hall A experimental setup are given in [8]; see [9] for further details of this experiment.

Throughout the experiment, singles  $^3\text{He}(e, e')$  quasi-elastic scattering data, measured simultaneously with coincidence  $^3\text{He}(e, e'p)$ , provided a continuous monitor of both luminosity and beam energy. The absolute normalization of our data was determined by comparing measurements of elastic scattering data to world data [10]. We measured the  $^3\text{He}(e, e'p)X$  cross section at three

beam energies, keeping  $|\vec{q}|$  and  $\omega$  fixed in order to separate response functions and understand systematic uncertainties. The data reported in this paper were all obtained at a beam energy of 4806 MeV.

The missing energy resolution, about 1 MeV ( $\sigma$ ), is less than the 2.23 MeV separation between the  ${}^3\text{He}(e, e'p)d$  peak and the threshold for the  ${}^3\text{He}(e, e'p)pn$  breakup channels. The radiative corrections to the measured cross sections were performed by using the code MCEEP [11]. The radiative tail is simulated and folded into the  $(E_m, p_m)$  space based on the prescription of Borie and Drechsel [12]. The radiative corrections in the continuum amount to 10 – 20% of the cross section. In particular, the radiative corrections remove the tail of the 2bbu process from the 3bbu data, allowing a clear separation of the channels. An exception is for low missing momentum, below 100 MeV/c, where the 3bbu strength is less than the strength of the radiative tail of the much stronger 2bbu peak.

Table I shows the central proton spectrometer settings for the experimental kinematics presented in this paper. The data taken at these settings are grouped into numerous  $(E_m, p_m)$  bins for presentation; Fig. 2 shows the cross sections corrected for radiative processes as a function of missing energy for several selected bins. The energy scale in the horizontal axis has been shifted in these plots so that the 3bbu channel starts at 0. As  $p_m$  increases, we can see that the broad peak in the cross section moves to higher missing energies. The arrow in the figure indicates where one would expect the peak in the cross section due to disintegration processes involving two active nucleons plus a spectator; the expected peak position for  $p_m = 820$  MeV/c is just off scale, at  $E_m \approx 145$  MeV. The large peak in the data roughly aligned with the arrow suggests that two-nucleon disintegration processes are dominant.

Several calculations are presented in Fig. 2. The simplest calculation is a plane-wave impulse approximation (PWIA) calculation using Salme's spectral function [13] and the  $\sigma_{cc1}$  electron-proton off-shell cross section [14]. Also shown in Fig. 2 are the results of microscopic calculations of the continuum cross section by J. M. Laget [15], including a PWIA calculation with correlations but

TABLE I: Proton spectrometer kinematic settings.

$p_m$ (MeV/c)	$P_p$ (MeV/c)	$\theta_p$ ( $^\circ$ )
150	1493	54.04
300	1472	59.83
425	1444	64.76
550	1406	69.80
750	1327	78.28
1000	1171	89.95

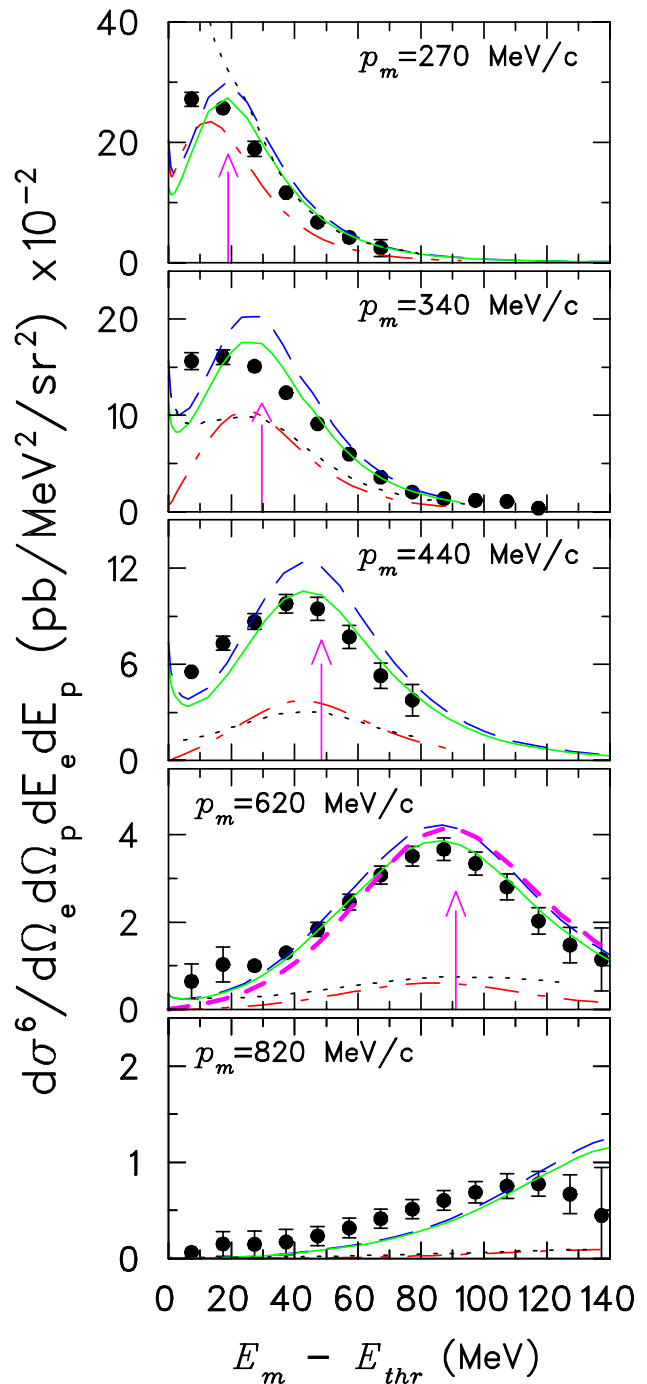


FIG. 2: (color online). Cross-section results for the  ${}^3\text{He}(e, e'p)pn$  reaction versus missing energy  $E_m$ . The vertical arrow gives the peak position expected for disintegration of correlated pairs. The dotted curve presents a PWIA calculation using Salme's spectral function and  $\sigma_{cc1}$  electron-proton off-shell cross section. Other curves are recent theoretical predictions of J. M. Laget [19] from the PWIA (dash dot) to PWIA + FSI (long dash) to full calculation (solid), including meson exchange current and final state interactions. In the 620 MeV/c panel, the additional short dash curve is a calculation with PWIA + FSI only within the correlated pair.

no FSI, and successive implementation of various interaction effects. The calculation is based on a diagrammatic expansion of the reaction amplitude, up to and including two loops [16]. Both single and double NN scattering, as well as meson exchange ( $\pi$  and  $\rho$ ) and  $\Delta$  formation are included. The bound-state wave function is a solution of the Faddeev equation used by the Hannover group [17] for the Paris potential [18]. Nucleon and meson propagators are relativistic and no angular approximations (Glauber) have been made in the various loop integrals. The FSI in these calculations use a global parameterization of the  $NN$  scattering amplitude, obtained from experiments at LANL, SATURNE and COSY [19]. Further details of the model can be found in [20].

Figure 2 shows that the calculated cross sections exhibit a correlation peak that is dominant at low  $p_m$ , but that FSI strongly enhance the cross section at large  $p_m$ . The calculations indicate the FSI are mainly between the two active nucleons – Fig. 1b. The additional calculation included in the 620 MeV/c panel of Fig. 2 has FSI with the spectator nucleon – Fig. 1c – turned off. Neither the shape nor magnitude of the peak is much affected. This result indicates that triple rescattering is negligible. MEC effects are also small.

To obtain the total 3bbu strength, and to facilitate comparison to the 2bbu, we divided the cross section by the elementary off-shell electron-proton cross section  $\sigma_{ep}$  [14], multiplied by a kinematic factor  $K$ , and integrated

over missing energy to obtain the effective momentum density distribution:

$$\eta(p_m) = \int \left( \frac{d^6\sigma}{dE_e dE_p d\Omega_e d\Omega_p} / K \sigma_{ep} \right) dE_m. \quad (2)$$

Figure 3 shows the distribution obtained. Uncertainties from missing tails of the 3bbu peak, within this integration range, due to limited experimental acceptance are negligible on the scale of Fig. 3. The 3bbu distribution tends to have a much larger relative strength for high missing momentum than does the 2bbu distribution – the ratio of 3bbu to 2bbu strength increases with  $p_m$  by about three orders of magnitude, from about 100 to 800 MeV/c. An increase of the relative strength with  $p_m$  is consistent with what is expected from correlations, as described in the simple picture in the introduction, but we already know from the discussion of Fig. 2 that FSI are important.

The PWIA curves in Fig. 3 show an order of magnitude enhancement of the 3bbu over the 2bbu at high missing momentum. The two-body correlations are more clearly seen in 3bbu than in the 2bbu since the available phase space is reduced when two nucleons are forced to form the deuteron. The differences between the PWIA calculations and full calculations further indicate the greater importance of final-state interactions in the 3bbu. Thus, the larger FSI in the 3bbu mask the larger role of correlations. The generally good agreement of the full calculations and the data shown in Figs. 2 and 3 relies mainly on the interplay of correlations and final-state interactions, and indicates no need for physics beyond that already present in a modern conventional nuclear physics model. The conclusions presented here have been confirmed by subsequent, independent calculations [21].

The conclusions described above might appear to be no longer valid for  $p_m \approx 1$  GeV/c as the magnitude of the 3bbu appears to fall towards that of the 2bbu. However, the center of the 3bbu correlation peak moves outside of the integration range at  $p_m \approx 800$  MeV/c, as shown in Fig. 2. Thus, the experimental integration only includes a fraction of the 3bbu strength at large  $p_m$ . A crude correction to account for the missing strength, using the fraction of strength of the full calculation of Laget in the region  $E_m < 140$  MeV, causes the 3bbu distribution to roughly flatten out, starting near 750 MeV/c, at a level nearly two orders of magnitude greater than that of the 2bbu. The large correction also leads to our stopping the calculation at 1 GeV/c; the comparison between data and theory is no longer meaningful when only a small fraction of the tail of the distribution is considered. Given these data along with the theoretical calculations, it remains fair to conclude that the correlations in the wave function preferentially lead to the 3bbu channel, and that the reaction mechanism is reasonably well understood in a modern, conventional nuclear physics model.

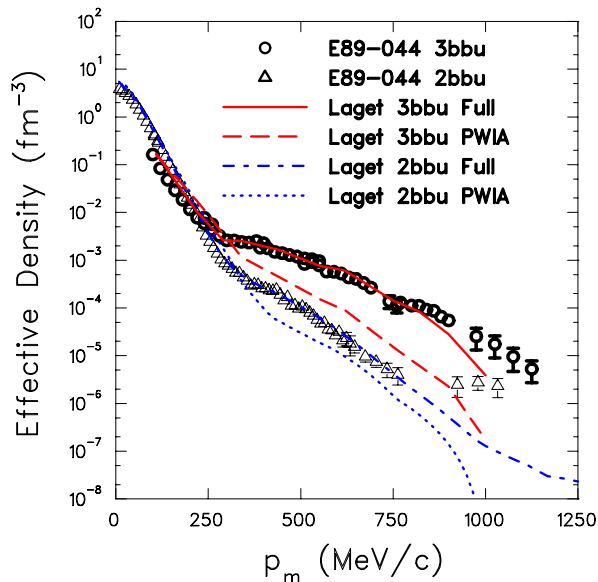


FIG. 3: (color online). Proton effective momentum density distributions in  ${}^3\text{He}$  extracted from  ${}^3\text{He}(e, e'p)pn$  (open black circles) and  ${}^3\text{He}(e, e'p)d$  (open black triangles), compared to calculations from Laget [19]. The 3bbu integration covers  $E_M$  from threshold to 140 MeV.

The comparison of the data of this experiment with the existing calculation suggests that the region near 300 MeV/ $c$  might prove to be the most enlightening with respect to the role of correlations. Here the full and PWIA curves are very similar to each other and to the data, and in the theory the correlation peak dominates the cross section. Separated response functions, which are possible with data from the other kinematics of this experiment, can provide us with more complete tests of the theory.

In summary, results for the cross section at constant  $\vec{q}$  and  $\omega$  have been presented for the  ${}^3\text{He}(e, e'p)pn$  reaction channel. The experimental data are both much higher in statistics and more extensive in kinematic coverage than any previous measurement. Model calculations are in good agreement with the data. We believe these are benchmark data which will serve to stimulate additional independent calculations, and help to define the role of correlations in nuclear structure.

We acknowledge the outstanding support of the staff of the Accelerator and Physics Divisions at JLab that made this experiment successful. This work was supported in part by the U.S. Department of Energy contract DE-AC05-84ER40150 Modification No. M175 under which the Southeastern Universities Research Association (SURA) operates the Thomas Jefferson National Accelerator Facility, other Department of Energy contracts, the U.S. National Science Foundation, the Italian Istituto Nazionale di Fisica Nucleare (INFN), the French Atomic Energy Commission and National Center of Scientific Research, the Natural Sciences and Engineering Research Council of Canada, and Grant-in-Aid for Scientific Research (KAKENHI) (No. 14540239) from the Japan Society for Promotion of Science (JSPS).

- 
- [1] N. Liyanage *et al.*, Phys. Rev. Lett. **86**, 5670 (2001).
  - [2] L. Frankfurt and M. Strikman, Phys. Rep. **76**, 215 (1981).
  - [3] J. M. Laget, Nucl. Phys. A **358**, 275 (1981).
  - [4] C. Marchand *et al.*, Phys. Rev. Lett. **60**, 1703 (1988).
  - [5] J. M. LeGoff *et al.*, Phys. Rev. C **50**, 2278 (1994); J.J. van Leeuwe *et al.*, Phys. Lett. B **523**, 6 (2001).
  - [6] Jefferson Lab Experiment E89-044, *Selected Studies of the  ${}^3\text{He}$  nucleus through electrodisintegration at High Momentum Transfer*, M. Epstein, A. Saha, and E. Voutier, spokespeople.
  - [7] M. Rvachev *et al.*, Phys. Rev. Lett. (to be published); Ph.D. thesis, Massachusetts Institute of Technology (2003).
  - [8] J. Alcorn *et al.*, Nucl. Inst. Meth. A **522**, 294 (2004); see also <http://hallaweb.jlab.org/equipment/HRS.html>.
  - [9] F. Benmokhtar, Ph.D. thesis, Rutgers University (2004).
  - [10] A. Amroun *et al.*, Nucl. Phys. A **579**, 596 (1994).
  - [11] See <http://www.physics.odu.edu/~ulmer/mceep/mceep.html>.
  - [12] E. Borie and D. Drechsel, Nucl. Phys. A **167**, 369 (1971).
  - [13] A. Kievsky, E. Pace, G. Salme and M. Viviani, Phys. Rev. C **56**, 64 (1997).
  - [14] T. DeForest, Nucl. Phys. A **392**, 232 (1983).
  - [15] J. M. Laget, Phys. Lett. B **151**, 325 (1985).
  - [16] J. M. Laget, Phys. Rep. **69**, 1 (1981).
  - [17] C. Hadjuk *et al.*, Nucl. Phys. A **369**, 321 (1981), and Nucl. Phys. A **405**, 581 (1983).
  - [18] M. Lacombe *et al.*, Phys. Lett. B **101**, 139 (1981).
  - [19] J. M. Laget, Few Body Syst. Supp. **15**, 171 (2003); J. M. Laget, Phys. Lett. B **609**, 49 (2005).
  - [20] J. M. Laget, Nucl. Phys. A **579**, 333 (1994).
  - [21] C. Ciofi degli Atti and L.P. Kaptari, Phys. Rev. C **71**, 024005 (2005).